Adaptive Processing with Frequency Diverse Distributed Apertures

Lorne Applebaum and Raviraj Adve
Dept. of Elec. and Comp. Eng., University of Toronto
10 King's College Road
Toronto, ON M5S 3G4, Canada

Contact Information:

Lorne Applebaum
Dept. of Elec. and Comp. Eng.,
University of Toronto,
Toronto, ON M5S 3G4 Canada
Tel: (416) 946 7350
Fax: (416) 946 8765
E-mail: *lorne.applebaum@utoronto.ca*

Please consider this paper for the student paper competition

I. Introduction

Recent research has indicated that frequency diversity combined with a large sparse array can result in an extremely narrow main beam while reducing the effect of grating lobes [1], [2]. These works illustrated the benefits of frequency diversity based on a preliminary data model provided in [1]. The system under consideration is a rectangular array of sub-apertures distributed over a relatively large area in the $x-y$ plane. Waveform diversity is achieved by frequency; each sub-aperture transmits at a unique frequency but each sub-aperture processes all frequencies. Recent research has shown that due to the sparsity of the elements the target and interference is within the Fresnel region of the array. The spatial steering vector is, therefore, associated with a look point, not look angle. Frequency diversity implies true time delays are required for beam steering.

This paper extends the model in [1] and continues to investigate the proposed system by illustrating issues faced when applying adaptive processing to systems with frequency diversity. Specifically, the issues addressed in this paper are the need to address phase decorrelation across frequencies, as well as the challenge and effects of estimating the clutter covariance matrix.

II. Technical Summary

Consider N sub-apertures distributed on the $x-y$ plane at points (x_n, y_n). Each aperture transmits on a carrier frequency f_n modulated with M linear-FM pulses within a coherent pulse interval (CPI). To focus on a look point (X_t, Y_t, Z_t) a delay is added to each element's transmitted signal. The true time delay for the n^{th} element is

$$\Delta T_n = \frac{\max\{D_n\} - D_n}{c},$$

where D_n is the distance between the n^{th} element and the look point, and c is the speed of light. The signal received by the i^{th} element can also be delayed by ΔT_i. Independently delaying the received signals allows the time associated with the look point range gate to be identical for all elements.

The signal transmitted by the n^{th} element is given by

$$s(t) = u(t)e^{j2\pi f_n t + j\psi_n}; u(t) = \sum_{m=0}^{M-1} u_p(t - mT_r), \tag{1}$$

where $u(t)$ is the complex envelope of M linear-FM pulses with pulse repetition interval (PRI) T_r and ψ_n is a random phase.

Consider a reflecting artifact (target or clutter) labelled by index l at (X_l, Y_l, Z_l), which is not necessarily the look point. The time taken for the signal to reach the artifact from the n^{th} transmitting element is $\tau_{nl}^{\text{Tx}} = \left(\sqrt{(x_n - X_l)^2 + (y_n - Y_l)^2 + Z^2}\right)/c$. Similarly, the signal takes $\tau_{il}^{\text{Rx}} = \left(\sqrt{(x_i - X_l)^2 + (y_i - Y_l)^2 + Z_l^2}\right)/c$ to travel from the artifact to the i^{th} receiver. Thus, received signal at element i is

$$r_{inl}(t) = A_{nl}u(t - \tau_{nl}^{\text{Tx}} - \tau_{il}^{\text{Rx}})e^{j2\pi(f_n + f_{dnl})(t - \tau_{nl}^{\text{Tx}} - \tau_{il}^{\text{Rx}})}, \tag{2}$$

where A_{nl} is a complex amplitude (with ψ_n absorbed into its random phase) and f_{dnl} is the doppler frequency induced by the motion of the artifact and is a function of carrier frequency. Note that, although the artifacts are not necessarily in the far field, as described in [1], they are assumed to be far enough that the doppler frequency seen by each element is approximately the same.

After down conversion, matched filtering and receiver delay, the signal from a single artifact becomes

$$x_{inl}(t) = A_{nl}e^{-j2\pi f_n \tau_{inl}} \sum_{m=0}^{M-1} e^{j2\pi f_{dnl} m T_r} \chi(t - mT_r - \tau_{inl} - \Delta T_i, f_{dnl}), \tag{3}$$

where $\tau_{inl} = \tau_{nl}^{\text{Tx}} + \tau_{il}^{\text{Rx}}$ and $\chi(t, f)$ is the ambiguity function of the linear-FM pulse.

Consider the processing of only the m^{th} pulse. To focus on the look point, the receiver will range gate in such a way that the temporal term of the ambiguity function is zero for an artifact at the look point. That is, for all artifacts $x_{inl}(t)$ is sampled at the time

$$t = mT_r + \tau_{Lin} + \Delta T_i,$$

where τ_{Lin} is the total travel time from the n^{th} transmitter to the look point to the i^{th} receiver of the signal. The sample for the m^{th} pulse is the sum of the contributions of all artifacts,

$$x_{inm} = \sum_l A_{nl} e^{-j2\pi f_n \tau_{inl}} e^{j2\pi f_{dnl} m T_r} \chi(\tau_{Lin} - \tau_{inl}, f_{dnl}). \tag{4}$$

Space-Time Adaptive Processing (STAP) functions by applying weights derived using the interference covariance matrix [3]. The applicability of STAP to the above model was tested using the optimal interference covariance matrix and an estimated covariance matrix. The examples presented also illustrate the importance of coherent processing across the multiple frequencies.

A. Signal Statistics

Although down conversion eliminates the carrier signals, the signal samples from different carriers are statistically orthogonal. This is a result of the phase ψ in Eqn. (1), as well as the phase of A_{nl} induced by reflection in Eqn. (2). These phases are assumed to be random and uncorrelated across the frequencies.

Since the signals from each frequency are orthogonal, STAP can be performed on them independently. As a result, length-MN spatial-temporal sample snapshots can be used with STAP rather than the length-N^2M vectors suggested in [1]. These snapshots are column vectors denoted by $\mathbf{x}$. The elements of the vector span the samples from the M pulses within a coherent pulse interval (CPI) for each of the N receiving sub-apertures. In the following sections, the subscripts indicating transmitting element will be dropped since it is understood independent and identical processing is performed at each frequency.

B. Interference Covariance Matrix

The optimal interference covariance matrix is given by $\mathbf{R}_c = E\left\{\mathbf{x}_c \mathbf{x}_c^H\right\}$, where $\mathbf{x}_c$ corresponds to the snapshot of the signal composed only of interfering artifacts, $\mathbf{x}_c^H$ is its conjugate transpose and $E\{\,\cdot\,\}$ denotes the expectation value [3]. Note that the target itself is considered an interfering artifact at all look points other than its location. If there are N_c clutter artifacts with independently random phases in A_l, then from Eqn. (4)

$$\left\{\mathbf{R}_c\right\}_{pq} = \sum_{l=1}^{N_c} |A_l|^2 \, e^{j2\pi f_n(\tau_{\alpha l} - \tau_{il})} e^{j2\pi f_{dl} T_r (m-\beta)} \chi(\tau_{Li} - \tau_{il}, f_{dl}) \chi^*(\tau_{L\alpha} - \tau_{\alpha l}, f_{dl}),$$

with the p^{th} element of $\mathbf{x}_c$ corresponding to the element i and pulse m and the q^{th} element corresponding to element α and pulse β. Note that $\mathbf{R}_c$ depends on the look point.

To estimate the covariance matrix, samples straddling the look point range gate are used. The signal in Eqn. (3) is sampled K times at $t_k = mT_r + \tau_{Lin} + \Delta T_i + kT_s$, where the integer $k \in [-\lceil K/2 \rceil, \lfloor K/2 \rfloor]$ and T_s is the sample period. The estimated interference covariance matrix $\hat{\mathbf{R}}_c$ is obtained in the usual manner [3].

With either the optimal or estimated matrix, modified sample matrix inversion (MSMI) statistic [3] is used for target detection.

C. Steering Vector

The steering vector $\mathbf{s}$ is defined by the look point and doppler bank frequency. The element of $\mathbf{s}$ corresponding to frequency n, sub-aperture i and pulse m has the value

$$s_{im} = e^{-j2\pi f_n \tau_{il}} e^{j2\pi f_d m T_r} \chi(0, f_d). \tag{5}$$

III. Numerical Simulations

This section presents preliminary results illustrating the consequences of uncorrelated phase and the impact of estimating the clutter covariance matrix. The final paper will include an example specifically illustrating the impact of the Fresnel region.

A. Simulation Scenario

The scenario, similar to that in [1], consisted of a 16 element array distributed uniformly over a $200\mathrm{m} \times 200\mathrm{m}$ grid in the $x-y$ plane. Above the array, was a target and interfering clutter. The target was modelled as a point reflector with a SNR of $10\mathrm{dB}$ while the clutter was modelled as a ball of random low power sources with a radius of $200\mathrm{m}$ with a centre separated, in the x-direction from the target by $800\mathrm{m}$. A summary of simulation parameters is shown in Table I.

TABLE I
Simulation Parameters

Parameter	Value
N	16
M	8
Up Chirp Bandwidth	10MHz
Up Chirp Duration	10μs
PRI	50μs
Inter-element Frequency Offset	100MHz
Target SNR	10dB
Target Velocity	$50\mathrm{m/s}$
Clutter INR	50dB
Target Location	$(476.9\mathrm{m}, -60.0\mathrm{m}, 200\mathrm{km})$

B. Consequences of Uncorrelated Phase

The use of frequency diversity results in the unsought effect of random phase. It was desired for the proposed system to increase the target's return over the interference by combining the frequency diverse transmitted signals. However, the random phase discussed in II-A diminishes this. As shown in Figure 1(a), the random phase has the effect of deteriorating the target signal at the target's look point. Figure 1(b) depicts the artificial scenario with coherent phase across all frequencies. The coherence magnifies the target's signal much more than the clutter's signal. Clearly, this result is expected, but illustrates an extremely crucial aspect of frequency diversity—without eliminating the phase decorrelation across frequency, frequency diversity may hurt rather than help!

C. Estimating $\mathbf{R}_c$

Estimating $\hat{\mathbf{R}}_c$ is a more practical application of STAP. The clutter scenario, however, poses a challenge to the estimation. In order for $\hat{\mathbf{R}}_c$ to be non-singular, at least NM samples must be used in the estimate. For an accurate representation of the clutter at least $2NM$ samples should be made [4]. However, with a sample period T_s of $25\mathrm{ns}$ and a clutter ball diameter of $400\mathrm{m}$ it is difficult to obtain enough samples representative of the clutter using the parameters given in Table I. Thus, simulations using an estimated $\hat{\mathbf{R}}_c$ had a single pulse in the CPI ($M = 1$).

Figure 2(a) illustrates a simulation using the estimated $\hat{\mathbf{R}}_c$. The scenario used has the edge of the clutter ball $20\mathrm{m}$ from the target. For comparison, Figure 2(b) illustrates a simulation of spatially homogeneous clutter with statistic equal to that seen in the original scenario's target look point. Furthermore, an ideal target statistic is assumed whereby the target signal occupies a single look point snapshot. From this ideal scenario, STAP with an estimated $\hat{\mathbf{R}}_c$ is performed. Thus, Figure 2(b) provides a best case scenario for estimated processing. For both scenarios, coherence across frequencies is applied.

In Figure 2(a), the clutter is attenuated. Furthermore, upon comparison with Figure 2(b), it is seen that the target's signal is attenuated. Nevertheless, target discrimination is possible.

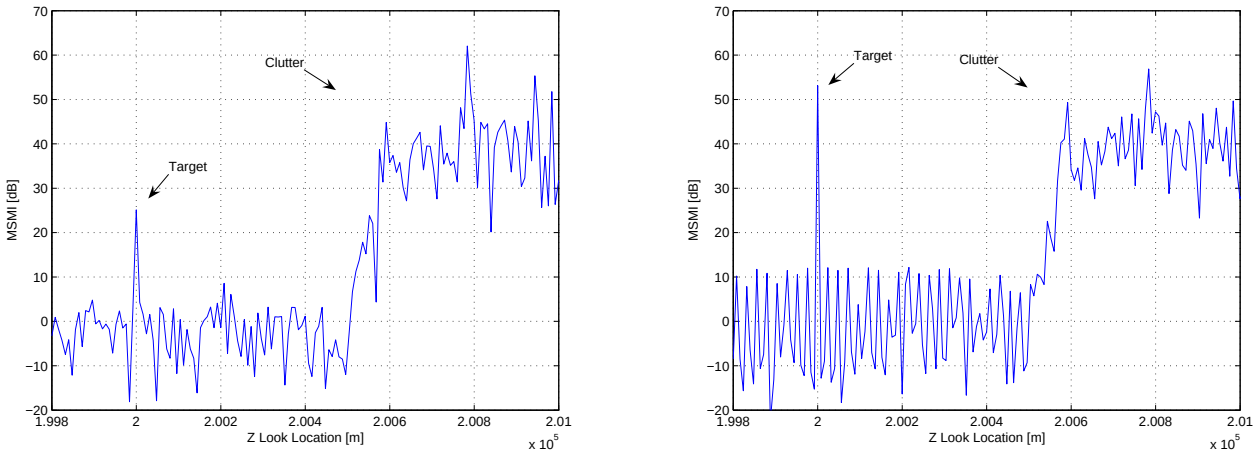

(a) With random phase

(b) Without random phase

Fig. 1. Simulations using optimal $\mathbf{R}_c$ illustrating the effects of random phase

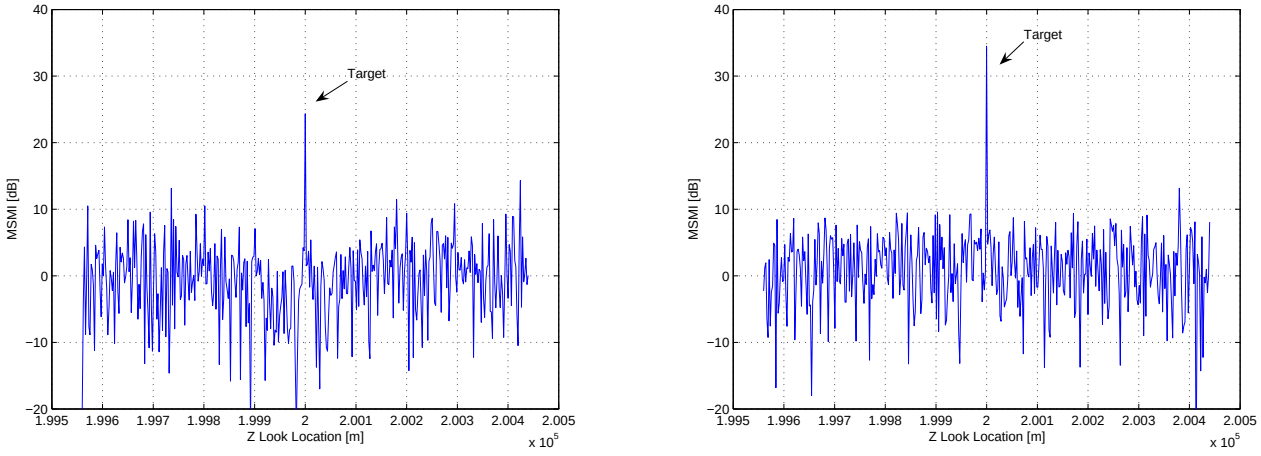

(a) Clutter ball scenario

(b) Spatially homogeneous clutter scenario

Fig. 2. Two simulations illustrating estimated processing

IV. Future Work

Due to time constraints, two topics that are planned for the final paper are absent from this summary. The final paper will address the effect of frequency diversity on grating lobes. Furthermore, comparisons between estimated and optimal processing will be included, addressing the effect of range dependence of the steering vector on clutter processing.

References

[1] R. Adve, R. Schneible, G. Genello, and P. Antonik, "Waveform-space-time adaptive processing for distributed aperture radars," in *Proc. of the 2005 IEEE International Radar Conference*, May 2005, pp. 93 – 97.

[2] R. S. Adve, R. Schneible, M. C. Wicks, and R. McMillan, "Adaptive processing for distributed aperture radars," in *Proc. of 1st Annual IEE Waveform Diversity Conference*, Nov. 2004, edinburgh.

[3] J. Ward, "Space-time adaptive processing for airborne radar," MIT Lincoln Laboratory, Tech. Rep., December 1994.

[4] I. S. Reed, J. Mallett, and L. Brennan, "Rapid convergence rate in adaptive arrays," *IEEE Transactions on Aerospace and Electronic Systems*, vol. 10, No. 6, pp. 853–863, Nov. 1974.